




Safety and efficacy of frameless stereotactic robot-assisted intraparenchymal brain lesion biopsies versus image-guided biopsies: a bicentric comparative study

Arthur Leclerc^{1,2} · Louise Deboeuf³ · Angela Elia^{3,4} · Oumaima Aboubakr³ · Martin Planet³ · Aziz Bedioui³ · Frédéric Rault¹ · Maxime Faisant⁵ · Alexandre Roux^{3,4} · Giorgia Antonia Simboli^{3,4} · Alessandro Moiraghi^{3,4} · Thomas Gaberel^{1,6} · Johan Pallud^{3,4} · Evelyne Emery^{1,6} · Marc Zanello^{3,4} 

Received: 4 October 2023 / Accepted: 6 November 2023

© The Author(s), under exclusive licence to Springer-Verlag GmbH Austria, part of Springer Nature 2024

Abstract

Purpose User-friendly robotic assistance and image-guided tools have been developed in the past decades for intraparenchymal brain lesion biopsy. These two methods are gradually becoming well accepted and are performed at the discretion of the neurosurgical teams. However, only a few data comparing their effectiveness and safety are available.

Methods Population-based parallel cohorts were followed from two French university hospitals with different surgical methods and defined geographical catchment regions (September 2019 to September 2022). In center A, frameless robot-assisted stereotactic intraparenchymal brain lesion biopsies were performed, while image-guided intraparenchymal brain lesion biopsies were performed in center B. Pre- and postoperative clinical, radiological, and histomolecular features were retrospectively collected and compared.

Results Two hundred fifty patients were included: 131 frameless robot-assisted stereotactic intraparenchymal brain lesion biopsies in center A and 119 image-guided biopsies in center B. The clinical, radiological, and histomolecular features were comparable between the two groups. The diagnostic yield (96.2% and 95.8% respectively; $p = 1.000$) and the overall postoperative complications rates (13% and 14%, respectively; $p = 0.880$) did not differ between the two groups. The mean duration of the surgical procedure was longer in the robot-assisted group (61.9 ± 25.3 min, range 23–150) than in the image-guided group (47.4 ± 11.8 min, range 25–81, $p < 0.001$). In the subgroup of patients with anticoagulant and/or antiplatelet therapy administered preoperatively, the intracerebral hemorrhage > 10 mm on postoperative CT scan was higher in the image-guided group (36.8%) than in the robot-assisted group (5%, $p < 0.001$).

Conclusion In our bicentric comparative study, robot-assisted stereotactic and image-guided biopsies have two main differences (shorter time but more frequent postoperative hematoma for image-guided biopsies); however, both techniques are demonstrated to be safe and efficient.

Keywords Neurosurgery · Neuropathology · Neuronavigation · Intraoperative complications · Postoperative complications · Postoperative period

Johan Pallud and Evelyne Emery participated equally. Previous presentations: There have been no reports of such data.

✉ Marc Zanello
m.zanello@ghu-paris.fr

¹ Department of Neurosurgery, Caen University Hospital, Caen, France

² UNICAEN, ISTCT/CERVOxy Group, UMR6030, GIP CYCERON, Normandy University, Caen, France

³ Service de Neurochirurgie, GHU Paris Psychiatrie et Neurosciences, Hôpital Sainte-Anne, 1, rue Cabanis, 75674, F-75014 Paris Cedex 14, France

⁴ Institute of Psychiatry and Neuroscience of Paris (IPNP), INSERM U1266, IMA-BRAIN, Université Paris Cité, 75014 Paris, France

⁵ Department of Anatomopathology, Caen University Hospital, Caen, France

⁶ UNICAEN, INSERM, U1237, PhIND “Physiopathology and Imaging of Neurological Disorders,” Institut Blood and Brain @ Caen-Normandie, Normandie University, Cyceron, Caen, France

Introduction

Intraparenchymal brain lesion biopsies are indicated for the diagnosis of various neurological conditions, including brain tumors, infections, and autoimmune diseases [15, 30]. In the past decades, biopsy procedures were commonly performed under stereotactic CT scan localization using a Leksell frame [7]. Two new technical approaches are gradually implemented in daily neurosurgical practice: frameless robot-assisted stereotactic biopsy [27, 32] and image-guided biopsy [21, 29]. Both techniques require trajectory planning. Frameless robot-assisted stereotactic biopsy is based on the use of a robotic arm to guide the biopsy cannula to the brain target, following the trajectory planned on preoperative MRI which will be fused with intraoperative CT scan controls [9, 10]. Image-guided biopsies use a navigation system including a computer-based image processing module, a reference frame, and a pointer tracked by an optical or electromagnetic detector, allowing for real-time navigation of the biopsy needle to the brain target [21]. Both techniques have been shown to be safe and effective in sampling intracranial lesions [8, 18, 21, 27, 32, 33].

Compared to historical framed-based stereotactic biopsies, several studies have shown both of these techniques to be equivalent in terms of efficacy and safety [5, 25, 28]. Nevertheless, the comparative effectiveness of frameless robot-assisted stereotactic intraparenchymal brain lesion biopsies versus image-guided biopsies has not been well established in clinical practice. To date, only one study compared the accuracy of both techniques to reach a predefined target in a small subset of patients but did not report clinical outcomes [20]. It could be challenging to design a prospective study comparing two surgical techniques due to each surgeon's team habits, various costly surgical tools required, and the learning curve necessary to be able to use the new method efficiently. However, it is possible to analyze two different daily practices from two centers with the same preoperative and postoperative protocols, by

determining control variables for population comparison in terms of age, sex, and major comorbidity [12].

In the present study, we compared the safety, efficacy, and diagnostic yield of frameless robot-assisted stereotactic versus image-guided intraparenchymal brain lesion biopsies in two different neurosurgical centers.

Methods

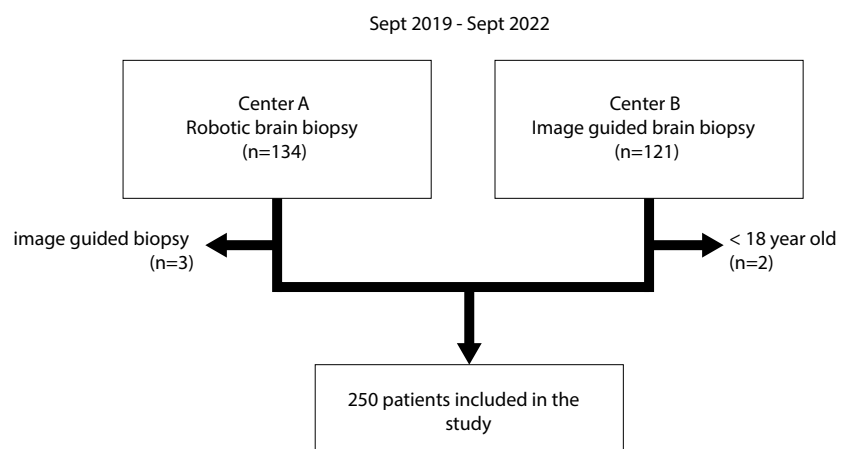
Study population

All consecutive adult patients > 18 years who had undergone biopsy for a newly diagnosed brain lesion between September 2019 and September 2022, at two French tertiary neurosurgical centers, were included in the present retrospective cohort study. Exclusion criteria were (1) extra-parenchymal intracranial lesion, (2) open brain lesion biopsy, and (3) previous surgery or oncological treatment. The inclusion flowchart is presented in Fig. 1.

Variables and data sources

The following data were systematically collected at the time of surgery using a dedicated table: age, sex, clinical symptoms, Karnofsky Performance Status (KPS) score, previous history of cancer, preoperative treatment (corticosteroid, antiplatelet, and/or anticoagulant therapies), tumor location, contrast enhancement, spontaneous hemorrhage within the lesion, cystic component, surgical duration (from head clamp positioning to end of closure), and type of neurosurgical procedure (frameless robot-assisted stereotactic biopsy or image-guided biopsy), number of biopsy trajectories, number of biopsy samples, occurrence of intraoperative bleeding from biopsy cannula, histomolecular diagnosis according

Fig. 1 Patient inclusion flow-chart



to the World Health Organization (WHO) classification of central nervous system (CNS) tumors 2021, immediate postoperative KPS score, and postoperative clinical (new neurological deficit, infection, and death) and imaging (postoperative hemorrhage, postoperative ischemia, increased mass effect) complications. The size of the postoperative intracerebral hematoma was quantified on the postoperative CT scan (performed the day after the surgery) by measuring the major axis of the hematoma on the axial plane.

Surgical procedures

Figures 2 and 3 illustrate the frameless robot-assisted stereotactic intraparenchymal brain lesion biopsy and the image-guided biopsy procedures, respectively (in each case, the patient consented to the publication of their image). Indications for intraparenchymal brain lesion biopsy were similar among both centers and defined according to French guidelines from the Association des Neuro-oncologues d'Expression Française [16]: (1) lesion ineligible for surgical resection, (2) tumor-like lesion confirmed on preoperative MRI, and (3) KPS score ≥ 50 . Both centers used the French guidelines from the Société Française d'Anesthésie-Réanimation concerning the intraoperative management of anticoagulant and antiplatelet therapy [11]. In both centers,

the biopsy trajectory was planned to avoid sulci and vessels. Center A performed frameless robot-assisted stereotactic biopsies with a NeuroMate Renishaw® minimally invasive robot, using a methodology previously detailed [33]. The biopsy trajectory was planned before surgery using the iPlan® software (Brainlab®, Munich, Germany). Under general anesthesia, the head was fixed using a Talairach head clamp. Preoperative MRI was merged with intraoperative 3D imaging acquired with the O-Arm, using the Neuroinspire software of the NeuroMate robot. This was done to align the biopsy cannula with the planned trajectory and to ensure its exact position at the target during the procedure. The cranial opening was made with a drill bit of 2.5 mm. Center B performed image-guided biopsies using the VarioGuide neuronavigation system (Brainlab®, Munich, Germany). The preoperative MRI was imported into an optical neuronavigation system (Curve Navigation, Brainlab®, Munich, Germany) for 3D reconstruction. The biopsy trajectory was performed directly on the curve module. Under general anesthesia, the head was fixed using a Mayfield skull clamp, and the reference array was connected to the head skull clamp. A 3D volume rendering of the patient's head was created through the infrared detector according to the interpolation of the reflective markers' position. The VarioGuide arm supporting the biopsy needle (Disposable Biopsy Needle, Brainlab®) was manually aligned to the planned trajectory

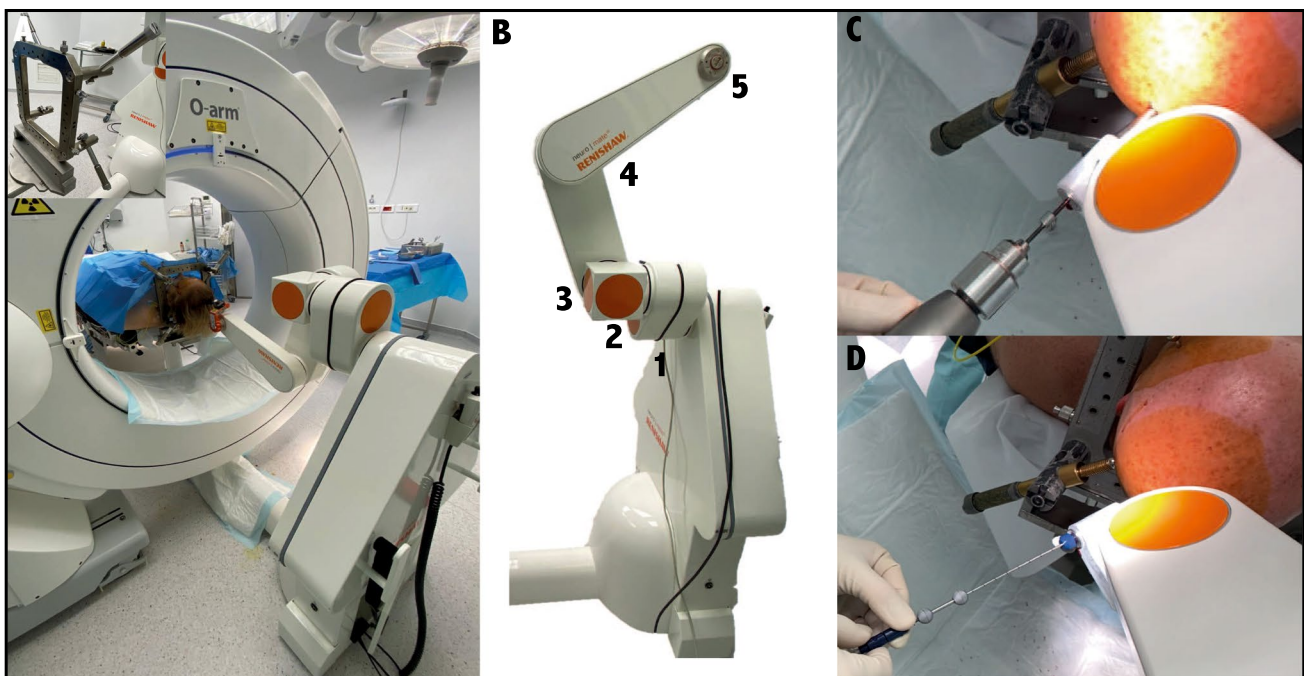


Fig. 2 Illustration of the frameless robot-assisted stereotactic brain biopsy. **A** Overview of the patient in prone position, his head in the Talairach head clamp fixed to the base of the robot, with the cone beam CT allowing frameless registration. In the top left corner, details of the Talairach head clamp. **B** Description of the five degrees

of freedom of the robotic arm (NeuroMate, Renishaw). **C** The drill hole is performed with a 2.5-mm diameter drill bit. **D** The 10-mm window side-cutting biopsy cannula is inserted, and its movements are controlled by the robot

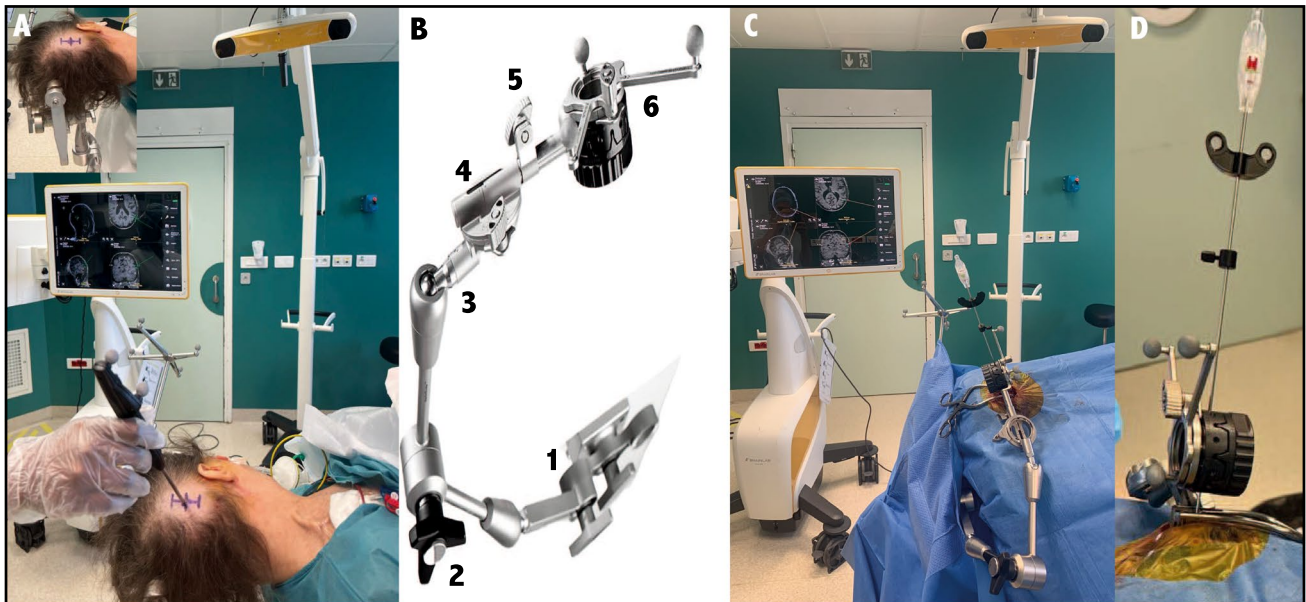


Fig. 3 Illustration of the image-guided brain biopsy. **A** Overview of the patient in prone position, his head in the Mayfield skull clamp with the reference star, allowing to calibrate the optical neuronavigation. In the top left corner, details of the Mayfield 3-pin skull clamp. **B** Description of the six degrees of freedom of the neuronavigation

arm (VarioGuide, BrainLab). **C** The drill hole is performed with a 14-mm diameter drill bit, and then, the joints of the neuronavigation arm are locked accordingly to the optical neuronavigation. **D** The 10-mm window side-cutting biopsy cannula is inserted, and its movements are controlled on the neuronavigation screen

by locking the six joints successively, and the biopsy needle was inserted to the target under optical control. The cranial opening was made with a self-stopping craniotomy drill bit of 14 mm.

Statistical analyses

Univariate analyses were carried out using Fisher's exact or chi-squared tests to compare categorical variables and using the Mann–Whitney rank-sum test or unpaired *t*-test for continuous variables, appropriately. Significance in univariate analysis was set at a *p*-value of <0.05. Analyses were performed by using the JMP software (Version 16.2.0; SAS Institute Inc, Cary, North Carolina, USA).

Standard protocol approvals, registrations, and patient consents

The authors have full access to the data and information presented for publication. The authors declare that they have no conflicts of interest. This study received the required authorizations (IRB#1:2023/10) from the institutional review board (IRB00011687). According to French legislation, the requirement for informed consent was waived for this observational retrospective study.

This manuscript was prepared in accordance with the Strengthening the Reporting of Observational Studies in Epidemiology (STROBE) checklist.

Results

Study population

During the inclusion period, 134 patients were treated in center A, and 121 patients were treated in center B. Three patients who underwent an image-guided biopsy in center A were excluded, and two patients aged < 18 years were excluded from center B. A total of 250 patients (60.8% of men, mean age 65.3 ± 13.5 years) were included in this study (Fig. 1): 131 patients in center A and 119 patients in center B.

Clinical, radiological, and histomolecular findings

Clinical, radiological, and histomolecular findings and group comparability (in terms of age, sex, and major comorbidity) are detailed in Table 1. The median preoperative KPS score was 80 (IQ, 70–90). The main presenting symptoms were neurological impairment (72.8%), followed by epileptic seizures (19.2%), signs of raised intracranial pressure (5.2%), and incidental discovery (2.8%). An anticoagulant and/or

Table 1 Clinical, radiological, histomolecular findings, and group comparability

| Parameters | Whole series (<i>n</i> = 250) | Center A Robotic biopsies (<i>n</i> = 131) | Center B Image-guided biopsies (<i>n</i> = 119) | <i>p</i> -value |
|--|--------------------------------|--|---|-----------------|
| Sex | | | | |
| Male | 152 (60.8%) | 74 (56.4%) | 78 (65.6%) | 0.142 |
| Female | 98 (39.2%) | 57 (43.6%) | 41 (34.4%) | |
| Age, years (mean ± SD) | 65.3±13.5 | 65.1±12.2 | 65.4±14.7 | 0.349 |
| KPS score (median, IQ) | 80 (70-90) | 80 (70-90) | 80 (60-90) | 0.838 |
| Symptoms at diagnosis | | | | |
| Neurological deficit | 182 (72.8%) | 88 (67.2%) | 94 (79%) | 0.189 |
| Epileptic seizures | 48 (19.2%) | 30 (22.9%) | 18 (15.1%) | |
| Intracranial hypertension | 13 (5.2%) | 9 (6.9%) | 4 (3.4%) | |
| Incidental discovery | 7 (2.8%) | 4 (3.6%) | 3 (2.5%) | |
| Anticoagulant and/or antiplatelet therapy | | | | |
| No | 191 (76.4%) | 91 (69.5%) | 100 (84%) | 0.018 |
| Yes | 59 (23.6%) | 40 (30.5%) | 19 (16%) | |
| Corticosteroid treatment | | | | |
| No | 143 (57.2%) | 75 (57.3%) | 68 (57.1%) | 0.986 |
| Yes | 107 (42.8%) | 56 (42.7%) | 51 (42.9%) | |
| Medical history of cancer | | | | |
| No | 212 (84.8%) | 107 (81.7%) | 105 (88.2%) | 0.147 |
| Yes | 38 (15.2%) | 24 (18.3%) | 14 (11.8%) | |
| Main location of the tumor | | | | |
| Lobar supratentorial | 198 (79.2%) | 109 (83.2%) | 89 (74.8%) | 0.212 |
| Basal ganglia | 40 (16%) | 17 (13%) | 23 (19.3%) | |
| Brainstem | 6 (2.4%) | 2 (1.5%) | 4 (3.4%) | |
| Cerebellar | 4 (1.6%) | 1 (0.8%) | 3 (2.5%) | |
| Pineal | 2 (0.8%) | 2 (1.5%) | 0 (0%) | |
| Cystic | | | | |
| No | 233 (93.2%) | 122 (93.1%) | 111 (93.2%) | 0.963 |
| Yes | 17 (6.8%) | 9 (6.9%) | 8 (6.8%) | |
| Spontaneously hemorrhagic | | | | |
| No | 234 (93.6%) | 122 (93.1%) | 112 (94.1%) | 0.749 |
| Yes | 16 (6.4%) | 9 (6.9%) | 7 (5.9%) | |
| Contrast enhancement | | | | |
| No | 42 (16.8%) | 20 (15.3%) | 22 (18.4%) | 0.496 |
| Yes | 208 (83.2%) | 111 (84.7%) | 97 (81.6%) | |
| Histomolecular diagnosis | | | | |
| WHO grade 4 glioma | 167 (66.8%) | 90 (68.7%) | 77 (64.7%) | 0.112 |
| WHO grade 3 glioma | 6 (2.4%) | 3 (2.3%) | 3 (2.5%) | |
| WHO grade 2 glioma | 4 (1.6%) | 1 (0.75%) | 3 (2.5%) | |
| WHO grade 1 glioma | 2 (0.8%) | 1 (0.75%) | 1 (0.9%) | |
| Unspecified glioma | 12 (4.8%) | 10 (7.6%) | 2 (1.7%) | |
| Lymphoma | 33 (13.2%) | 11 (8.4%) | 22 (18.5%) | |
| Metastasis | 7 (2.8%) | 4 (3%) | 3 (2.5%) | |
| Inflammatory or infectious process | 9 (3.6%) | 6 (4.6%) | 3 (2.5%) | |
| Negative | 10 (4%) | 5 (3.8%) | 5 (4.2%) | |
| Histomolecular diagnosis | | | | |
| No | 10 (4%) | 5 (3.8%) | 5 (4.2%) | 0.877 |
| Yes | 240 (96%) | 126 (96.2%) | 114 (95.8%) | |
| Histomolecular diagnosis in patients with deep-seated lesion* (<i>n</i> = 48) | | | | |
| No | | <i>n</i> = 21 2 (4%) | <i>n</i> = 27 0 (0%) | 0.116 |
| Yes | | 19 (96%) | 100 (100%) | |

KPS Karnofsky Performance Status, IQ interquartile, SD standard deviation, WHO World Health Organization

*Deep seating lesion includes the brainstem, pineal gland, and basal ganglia

antiplatelet therapy, which was stopped 5 days preoperatively according to the guidelines of the French National Health Agency [6], was preoperatively administered to 24.4% of patients (antiplatelet therapy only in 16%, both in 8.4%). Preoperative corticosteroid treatment was administered without discontinuation until surgery (mean duration 6.7 ± 14.9 days, range 0–150; mean dose 28.9 ± 38.7 mg/day, range 0–200) to 42.8% of patients. Thirty-eight patients (15.2%) had a medical history of cancer. The main lesion location was supratentorial and lobar in 79.2% of cases, deep-seated (i.e., brainstem, pineal gland, and basal ganglia) in 19.2% of cases, and cerebellar in 1.6% of cases. The lesion presented contrast enhancement in 83.2% of cases, was cystic in 6.8% of cases, and was spontaneously hemorrhagic in 6.4% of cases. Clinical and radiological findings did not significantly differ between the two centers ($p > 0.05$), except for the anticoagulant and/or antiplatelet therapy administration that was more frequent in patients from center A (30.5%) than from center B (16%, $p = 0.018$).

A conclusive histomolecular diagnosis was obtained in 96.0% of cases, and the diagnosis of glioblastoma *IDH*-wildtype CNS WHO grade 4 was the most common diagnosis (66.8%). The diagnostic yield did not significantly differ between centers ($p = 0.877$), even in the subgroup of patients with a deep-seated lesion ($p = 0.116$).

Intraoperative findings

Intraoperative findings and comparisons between techniques are detailed in Table 2. The mean duration of the surgical procedure (55.0 ± 21.3 min, range 23–150) was longer in center A (61.9 ± 25.3 min, range 23–150) than in center B (47.4 ± 11.8 min, range 25–81, $p < 0.001$). No procedure aborted. In all but two patients, one biopsy trajectory was performed (99.2%). In one patient from center A, two trajectories were performed: the first to sample the

lesion and the second to drain a tumoral cyst. In one patient from center B, a second trajectory was performed because the first samples did not appear abnormal on visual inspection. The median number of biopsy samples (8, IQ 6–8) was higher in center B (8, IQ 8–8) than in center A (6, IQ 4–8, $p < 0.001$). Intraoperative bleeding from biopsy cannula occurred in 4.4% of cases: 3.8% in center A and 5% in center B.

Postoperative outcomes

Postoperative outcomes and comparisons between techniques are detailed in Table 3. The median preoperative KPS score was 80 (IQ, 70–90), similar between center A (80, IQ 70–90) and center B (80, IQ 60–90, $p = 0.21$).

Early postoperative CT scan was performed at a mean of 1.5 ± 1.3 days post-operatively (range 0–11) in all but eight patients: eight patients of center B did not have early postoperative imaging due to good clinical condition and so were excluded from statistical analysis regarding postoperative hematoma. A postoperative hemorrhage > 10 mm in diameter was observed in 10% of cases and was observed in 15.3% of cases in the subgroup of patients with an anticoagulant and/or antiplatelet therapy administration preoperatively. In the subgroup of patients with an anticoagulant and/or antiplatelet therapy preoperatively, a postoperative hemorrhage > 10 mm in diameter was observed more frequently in center B (36.8%) than in center A (5.0%, $p = 0.001$). The mean duration of hospital stays (4.0 ± 4.9 days, range 0–34) was longer in center B (4.9 ± 5.5 days, range 0–34) than in center A (3.1 ± 4.1 days, range 1–34, $p < 0.001$).

Thirty-four patients (13.6%) presented with postoperative complications: 9.2% presented with a worsened neurological deficit that remained permanent in 4% of cases, 3.6% presented with signs of increased intracranial pressure requiring osmotherapy, 3.2% presented with postoperative epileptic

Table 2 Intraoperative findings and comparison between techniques

| Parameters | Whole series ($n = 250$) | Center A | Center B | p -value |
|--|----------------------------|--------------------------------|-------------------------------------|-------------------|
| | | Robotic biopsies ($n = 131$) | Image-guided biopsies ($n = 119$) | |
| Duration of the surgical procedure: min (median, IQ) | 55.0 ± 21.3 | 61.9 ± 25.3 | 47.4 ± 11.8 | < 0.001 |
| Number of trajectories | | | | |
| 1 | 247 (98.8%) | 129 (98.4%) | 117 (99.2%) | 0.99 |
| 2 | 3 (1.2%) | 1 (1.6%) | 1 (0.8%) | |
| Number of biopsy samples (mean \pm SD) | 8 (6–8) | 6 (4–8) | 8 (8–8) | < 0.001 |
| Intraoperative bleeding | | | | |
| No | 241 (95.6%) | 126 (96.2%) | 113 (95%) | 0.637 |
| Yes | 9 (4.4%) | 5 (3.8%) | 6 (5%) | |

SD standard deviation

Table 3 Postoperative outcomes and comparison between techniques

| Parameters | Whole series (<i>n</i> = 250) | Center A Robotic biop- sies (<i>n</i> = 131) | Center B Image-guided biopsies (<i>n</i> = 119) | <i>p</i> -value |
|--|--------------------------------|---|--|-----------------|
| Postoperative KPS score (median, IQ) | 80 (70–90) | 80 (70–90) | 80 (60–90) | 0.21 |
| Postoperative hemorrhage > 10 mm* | | | | |
| No | 225 (90%) | 120 (91.6%) | 96 (87.3%) | 0.271 |
| Yes | 25 (10%) | 11 (8.4%) | 14 (12.7%) | |
| Postoperative hemorrhage > 10 mm* in subgroup of patients with anticoagulant and/or antiplatelet therapy administration (<i>n</i> = 59) | | <i>n</i> = 40 | <i>n</i> = 19 | |
| No | 52 (85.2%) | 38 (95%) | 12 (63.2%) | <0.001 |
| Yes | 9 (14.8%) | 2 (5%) | 7 (36.8%) | |
| Postoperative complication | | | | 0.76 |
| No | 216 (86.4%) | 114 (87%) | 102 (85.7%) | |
| Yes | 34 (13.6%) | 17 (13%) | 17 (14.3%) | |
| New/worsening of neurological deficit | | | | |
| No | 227 (90.8%) | 120 (91.6%) | 107 (89.9%) | 0.64 |
| Yes | 23 (9.2%) | 11 (8.4%) | 12 (10.1%) | |
| Permanent neurological deficit | | | | |
| No | 240 (96%) | 124 (94.7%) | 116 (97.5%) | 0.34 |
| Yes | 10 (4%) | 7 (5.3%) | 3 (2.5%) | |
| Intracranial hypertension | | | | |
| No | 241 (96.4%) | 128 (97.7%) | 113 (95%) | 0.31 |
| Yes | 9 (3.6%) | 3 (2.3%) | 6 (5%) | |
| Postoperative epileptic seizure | | | | |
| No | 242 (96.8%) | 125 (95.4%) | 117 (98%) | 0.29 |
| Yes | 8 (3.2%) | 6 (4.6%) | 2 (2%) | |
| Hematoma requiring surgical evacuation | | | | |
| No | 248 (99.2%) | 129 (98.5%) | 119 (100%) | 0.18 |
| Yes | 2 (0.8%) | 2 (1.5%) | 0 (0%) | |
| Infection | | | | |
| No | 248 (99.2%) | 130 (99.3%) | 118 (99.2%) | 1 |
| Yes | 2 (0.8%) | 1 (0.7%) | 1 (0.8%) | |
| General complication | | | | |
| No | 245 (98%) | 127 (96.9%) | 118 (99.1%) | 0.25 |
| Yes | 5 (2%) | 4 (3.1%) | 1 (0.9%) | |
| Death during the first postoperative month | | | | |
| No | 242 (96.8%) | 125 (95.4%) | 117 (98.3%) | 0.29 |
| Yes | 8 (3.2%) | 6 (4.6%) | 2 (1.7%) | |

KPS Karnofsky Performance Status

*Measured on postoperative CT scan

seizures that were not present preoperatively, 2.0% presented with general complications (two thromboembolic event, two pulmonary infections, one urinary infection), 0.8% presented a postoperative intracerebral hematoma requiring surgical evacuation, and 0.8% presented a postoperative surgical site infection. Overall, 3.2% of patients died during the first postoperative month. The overall rate of postoperative complications did not differ between groups ($p = 0.76$) nor did the rates of any specific complication (Table 3).

Discussion

Key results

In this bicentric retrospective study which included 250 patients who underwent a brain biopsy for a brain lesion by comparing frameless robot-assisted stereotactic biopsies (center A, 131 patients) versus image-guided biopsies (center B, 119 patients), it was demonstrated that (1) both

neurosurgical procedures were safe with low and similar complications rates, (2) both neurosurgical procedures were efficient with a similar diagnostic yield of 96%, (3) the duration of the procedure was shorter using image-guided intraparenchymal brain lesion biopsies than using frameless robot-assisted stereotactic biopsies, and (4) the rate of postoperative hemorrhage > 10 mm in diameter was higher using image-guided biopsies than using frameless robot-assisted stereotactic biopsies, in the subgroup of patients with an anticoagulant and/or antiplatelet therapy administration.

Interpretation

Image-guided and robot-assisted biopsies have gradually replaced frame-based stereotactic biopsies for intraparenchymal brain lesions. Image-guided biopsies use classical and user-friendly tools, i.e., optical neuronavigation, at the expense of a loss of accuracy [20]. This lower accuracy may be due to registration errors, distortions in MRI, or lack of rigidity of the skull clamp [24, 26]. By contrast, the more expensive (in comparison with optical neuronavigation) surgical robot used by center A provided better trajectory accuracy but required a longer learning curve [4]. The surgical accuracy of the rigid robotic arm using bone registration has been measured ranging from 0.59–0.7 mm, which is superior to that of frame-based biopsies [8, 9, 19]. In comparison, the surgical accuracy of a neuronavigation system such as the one used by center B has been measured ranging from 1.8–2.2 mm [10]. Robot-assisted stereotactic biopsy procedures frequently require intraoperative imaging acquisitions, allowing for intraoperative check of the accuracy of the actual biopsy trajectory [33]. This explains the longer duration of the surgical procedure we observed in the frameless robot-assisted stereotactic biopsy center [8, 33]. The surgical accuracy may impact the efficacy of the surgical procedure, but we reported similar diagnostic yields between the two techniques. The high diagnostic yield (96%) is consistent with previous series ranging from 98–99% [1, 21, 23] for frameless robot-assisted stereotactic intraparenchymal brain lesion biopsies and ranging from 96.6–100% [3, 17, 18, 27] for image-guided biopsies. Of particular interest, the diagnostic yield of the two procedures remained similar in the subgroup of patients harboring a deep-seated lesion, recalling a previous series of pediatric brainstem biopsies using a neuronavigation system [13]. This suggests that if the neurosurgical procedure is performed properly, whichever the technology of biopsy guidance, the diagnostic yield is excellent. Persisting causes of failure remained poor planning or a “pathological” cause, including the preoperative administration of corticosteroids in patients harboring a CNS lymphoma [2, 14].

We reported a 13% rate of post-biopsy complications in the present series encompassing general, major, and minor

postoperative events. We reported a 1% rate of postoperative intracerebral hemorrhage requiring surgical evacuation, which is consistent with previous series [5, 18, 21, 27]. We screened systematically for intracerebral hematoma, independently from their clinical relevance, on early postoperative imaging, and observed a lower prevalence of postoperative intracerebral hematoma > 10 mm in diameter, after frameless robot-assisted stereotactic biopsies compared to those after image-guided biopsies, in those patients who received a preoperative administration of an anticoagulant and/or antiplatelet therapy. This cannot simply be related to the different number of biopsy samples between centers A and B: according to previous studies, there is no correlation between the number of biopsy samples and postoperative hemorrhage [32]. This can reflect a significant difference in trajectory planning, which is a key step in stereotactic biopsy: while the neurosurgical team in center A performs a two-step neurosurgical planning, the neurosurgical team in center B performs the planning in the operating room, shortly before surgery [31]. This difference in terms of postoperative intracerebral hematoma suggests using preferentially the frameless robot-assisted stereotactic biopsy procedure in the population at risk of postoperative intracerebral hemorrhage. The 1-month 3% mortality rate we reported is similar to that reported in other intraparenchymal brain lesion biopsy series whatever the neurosurgical technique and is related to the evolution of the disease rather than a surgically induced event [21, 22, 27].

Generalizability

The present study selected a homogeneous population of adult patients harboring a newly diagnosed brain lesion operated on with two different neurosurgical procedures. This is the first study comparing the efficacy and the safety of frameless robot-assisted stereotactic biopsies versus image-guided biopsies using a retrospective bicentric design. We analyzed data provided from a daily practice: our study is a result of a naturally occurring experiment of different management strategies in two tertiary French centers. The French healthcare system ensured comparable study populations. The present results support the use of these two neurosurgical procedures to perform a biopsy of brain lesions in adults.

Limitations

These findings should be interpreted with caution, given the retrospective design and the exploratory design of the statistical analyses limiting the generalizability of the results. The original design (comparison between two neurosurgical centers favoring a particular biopsy procedure) limited selection biases (the practitioner was not tempted to favor

one technique or another based on experience, preference, or tumor characteristics). Nevertheless, this may have led to a lack of comparability between groups, especially considering the use of antithrombotic/anticoagulant treatment, possibly leading to statistical biases. Further confirmatory analyses are required to reproduce the present results.

Conclusions

In this original bicentric retrospective study, we have shown that frameless robot-assisted stereotactic and image-guided intraparenchymal brain lesion biopsies are both safe and efficient techniques. The two techniques are comparable, except with regards to operating time (shorter with image-guided biopsies) and the presence of a hematoma > 10 mm in patients on early postoperative CT scan in the subgroup of patients with anticoagulant and/or antiplatelet therapy (higher with image-guided biopsies).

Code availability Not applicable.

Data availability Data is available under request, according to owner protocols.

Declarations

Conflict of interest None.

References

1. Æbelø AM, Noer VR, Schulz MK, Kristensen BW, Pedersen CB, Poulsen FR (2019) Frameless stereotactic neuronavigated biopsy: a retrospective study of morbidity, diagnostic yield, and the potential of fluorescence: a single-center clinical investigation. *Clin Neurol Neurosurg* 181:28–32
2. Aliouat I, Moiraghi A, Simboli GA et al (2022) Accuracy and safety of 101 consecutive neurosurgical procedures for newly diagnosed central nervous system lymphomas: a single-institution experience. *J Neuro-Oncol*. <https://doi.org/10.1007/s11060-022-04069-6>
3. Bekelis K, Radwan TA, Desai A, Roberts DW (2012) Frameless robotically targeted stereotactic brain biopsy: feasibility, diagnostic yield, and safety. *J Neurosurg* 116(5):1002–1006
4. Bichsel O, Oertel MF, Stieglitz LH (2021) Mobile intraoperative CT-assisted frameless stereotactic biopsies achieved single-millimeter trajectory accuracy for deep-seated brain lesions in a sample of 7 patients. *BMC Neurol* 21(1):285
5. Dammers R, Haitsma IK, Schouten JW, Kros JM, Avezaat CJJ, Vincent AJPE (2008) Safety and efficacy of frameless and frame-based intracranial biopsy techniques. *Acta Neurochir* 150(1):23–29
6. de Santé HA (2008) Good management practices for oral anticoagulant overdose, situations of hemorrhagic risk and hemorrhagic events in patients taking oral anticoagulants in the ambulatory and hospital setting--April 2008. *J Mal Vasc* 33(4–5):202–213
7. Debaene A, Gomez A, Lavieille J, Alessandri C, Legre J (1988) Stereotactic CT localization and biopsy of brain tumours using the Leksell frame. A study of 45 cases. *J Neuroradiol* 15(3):266–275
8. Deboeuf L, Moiraghi A, Debacker C et al (2023) Feasibility and accuracy of robot-assisted, stereotactic biopsy using 3-dimensional intraoperative imaging and frameless registration tool. *Neurosurgery* 92(4):803–811
9. Faria C, Erlhagen W, Rito M, De Momi E, Ferrigno G, Bicho E (2015) Review of robotic technology for stereotactic neurosurgery. *IEEE Rev Biomed Eng* 8:125–137
10. Giese H, Hoffmann K-T, Winkelmann A, Stockhammer F, Jallo GI, Thomale U-W (2010) Precision of navigated stereotactic probe implantation into the brainstem. *J Neurosurg Pediatr* 5(4):350–359
11. Godon A, Albaladejo P (2019) Gestion périopératoire des anticoagulants. *J Med Vasc* 44(2):99
12. Jakola AS, Myrnel KS, Kloster R, Torp SH, Lindal S, Unsgård G, Solheim O (2012) Comparison of a strategy favoring early surgical resection vs a strategy favoring watchful waiting in low-grade gliomas. *JAMA* 308(18):1881–1888
13. Joud A, Stella I, Klein O (2020) Diffuse infiltrative pontine glioma biopsy in children with neuronavigation, frameless procedure: a single center experience of 10 cases. *Neurochirurgie* 66(5):345–348
14. Kan E, Levi I, Benharroch D (2011) Alterations in the primary diagnosis of lymphomas pretreated with corticosteroid agents. *Leuk Lymphoma* 52(3):425–428
15. Karasin B, Hardinge T, Eskuchen L, Watkinson J (2022) Care of the patient undergoing robotic-assisted brain biopsy with stereotactic navigation: an overview. *AORN J* 115(3):223–236
16. Laigle-Donadey F, Metellus P, Guyotat J et al (2023) Surgery for glioblastomas in the elderly: an Association des Neuro-oncologues d'Expression Française (ANOCEF) trial. *J Neurosurg* 138(5):1199–1205
17. Lefranc M, Capel C, Pruvot AS, Fichten A, Desenclos C, Tous-saint P, Le Gars D, Peltier J (2014) The impact of the reference imaging modality, registration method and intraoperative flat-panel computed tomography on the accuracy of the ROSA® stereotactic robot. *Stereotact Funct Neurosurg* 92(4):242–250
18. Lefranc M, Capel C, Pruvot-Ocean A-S, Fichten A, Desenclos C, Toussaint P, Le Gars D, Peltier J (2015) Frameless robotic stereotactic biopsies: a consecutive series of 100 cases. *J Neurosurg* 122(2):342–352
19. Li QH, Zamorano L, Pandya A, Perez R, Gong J, Diaz F (2002) The application accuracy of the NeuroMate robot--a quantitative comparison with frameless and frame-based surgical localization systems. *Comput Aided Surg* 7(2):90–98
20. Minchev G, Kronreif G, Ptacek W, Kettenbach J, Micko A, Wurzer A, Maschke S, Wolfsberger S (2020) Frameless stereotactic brain biopsies: comparison of minimally invasive robot-guided and manual arm-based technique. *Oper Neurosurg (Hagerstown)* 19(3):292–301
21. Mongardi L, Belaroussi Y, Kara M et al (2023) When to discharge patients following a neuronavigation-assisted brain biopsy for supratentorial lesion? A single-center experience. *Clin Neurol Neurosurg* 229:107727
22. Riche M, Marijon P, Amelot A et al (2022) Severity, timeline, and management of complications after stereotactic brain biopsy. *J Neurosurg* 136(3):867–876
23. Shooman D, Belli A, Grundy PL (2010) Image-guided frameless stereotactic biopsy without intraoperative neuropathological examination. *J Neurosurg* 113(2):170–178
24. Spetzger U, Hubbe U, Struffert T, Reinges MHT, Krings T, Krombach GA, Zentner J, Gilsbach JM, Stiehl HS (2002) Error analysis in cranial neuronavigation. *Minim Invasive Neurosurg* 45(1):6–10
25. Spyrtantis A, Wobbecke T, Constantinescu A, Cattani A, Quick-Weller J, Willems LM, Marquardt G, Seifert V, Freiman TM (2021) Comparison of frame-less robotic versus frame-based stereotactic biopsy of intracranial lesions. *Clin Neurol Neurosurg* 207:106762

26. Tavares WM, Tustumi F, da Costa LC, Gamarra LF, Amaro E, Teixeira MJ, Fonoff ET (2014) An image correction protocol to reduce distortion for 3-T stereotactic MRI. *Neurosurgery* 74(1):121–126 discussion126-127
27. Terrier L, Gilard V, Marguet F, Fontanilles M, Derrey S (2019) Stereotactic brain biopsy: evaluation of robot-assisted procedure in 60 patients. *Acta Neurochir* 161(3):545–552
28. Ungar L, Nachum O, Zibly Z et al (2022) Comparison of frame-based versus frameless image-guided intracranial stereotactic brain biopsy: a retrospective analysis of safety and efficacy. *World Neurosurg* 164:e1–e7
29. Wang X, Li L, Luo P, Li L, Cui Q, Wang J, Jing Z, Wang Y (2016) Neuronavigation-assisted trajectory planning for deep brain biopsy with susceptibility-weighted imaging. *Acta Neurochir* 158(7):1355–1362
30. Yogendran LV, Kalelioglu T, Donahue JH et al (2022) The landscape of brain tumor mimics in neuro-oncology practice. *J Neuro-Oncol* 159(3):499–508
31. Zanello M, Roux A, Debacker C et al (2021) Postoperative intracerebral haematomas following stereotactic biopsies: poor planning or poor execution? *Int J Med Robot* 17(2):e2211
32. Zanello M, Roux A, Senova S et al (2021) Robot-assisted stereotactic biopsies in 377 consecutive adult patients with supratentorial diffuse gliomas: diagnostic yield, safety, and postoperative outcomes. *World Neurosurg* 148:e301–e313
33. Zanello M, Simboli GA, Carron R, Pallud J (2022) MRI-based and robot-assisted stereotactic biopsy with intraoperative CT imaging. *Acta Neurochir* 164(12):3311–3315

Publisher's Note Springer Nature remains neutral with regard to jurisdictional claims in published maps and institutional affiliations.

Springer Nature or its licensor (e.g. a society or other partner) holds exclusive rights to this article under a publishing agreement with the author(s) or other rightsholder(s); author self-archiving of the accepted manuscript version of this article is solely governed by the terms of such publishing agreement and applicable law.